Emerging Application of a Structural and Chemical Analyser for the Complete Characterization of Metal-Rich Particulate Matter

Naiara Goienaga[*], *Alfredo Sarmiento, Maitane Olivares, Jose Antonio Carrero, Luis A. Fernández, Juan M. Madariaga*

[*] e-mail: naiara.goyenaga@ehu.es; Phone-number: +34.601.5551; Fax-number: +34.6013500

Department of Analytical Chemistry, University of the Basque Country (UPV/EHU), P.O. Box 644, E-48080, Bilbao, Basque Country, Spain

ABSTRACT:

Clean air is considered to be a basic requirement of human health and well-being. An increasing range of adverse health effects has been linked to air pollution, at ever-lower concentrations. This research shows the newly developed Structural and Chemical Analyzer (SCA) to be a successful combination of Raman spectroscopy and SEM-EDX that opens up new insight into the composition of Particulate Matter (PM). The results obtained with soil and lichen samples demonstrate the capability of the technique to obtain elemental and molecular information of every single atmospheric PM focused at the micron and submicron levels. The SCA analysis permitted the individual PM analysis, allowing the identification of the molecular (most commonly as sulphides, sulphates, carbonates or oxides) form in which several hazardous metals (Zn, Pb, Cu, etc.) are evolved into potentially inhalable PMs. During the present research, the synchronization of both techniques revealed the morphological, elemental and molecular forms of metal-rich PMs at a time, avoiding some analysis precautions and making more dynamic the sample preparation and measurement steps. In addition, the thermodynamic simulations carried out with the information obtained were helpful to differentiate whether the PM may be retained in the alveoli (i.e., galena) or if it may be dissolved and pass into the bloodstream (i.e., plattnerite).

INTRODUCTION

In recent decades, air quality has become a very important concern as more and more studies have shown the great impact of atmospheric pollution on environment (i.e., effects on agricultural and natural ecosystems), global climate change and human health[1].

Unlike other air pollutants (i.e., O_3, CO, SO_x, NO_x, organic pollutants), particulate matter (PM) is not a specific chemical entity. Airborne PM, which is a very complex and heterogeneous mixture of particles, composed of a broad class of chemically and physically diverse substances are changeable in size, chemical composition, formation, origin, and concentration; and are variable across space and time[2,3]. The shape and composition of PM is determined by its emission sources as well as by chemical reactions within the atmosphere. On the one hand, they can be directly emitted (primary PM) from natural sources or released from anthropogenic processes [4]. On the other hand, PM may be formed in the atmosphere (secondary PM) by gas-to-particle adsorption process and complex chemical reactions[5]. PM can also be produced from secondary oxidation in transit or be washed out of the atmosphere during precipitation events[6].

The characterization of the fine fractions of PMs (PM10, PM2.5 and PM1) represents an interesting field of investigation[7-9]. Many time-series studies have shown that air pollution PM is associated with an increased risk of diseases and even death from cardiovascular and/or respiratory causes in both Europe and the USA[10-12]. Specially, ultrafine PM which provide high surface area-to-volume ratio may lead to higher toxicity on human health because it is able to go deeper in the human respiratory track[13,14]. In consequence, PM size has commonly been the most available metric used in epidemiology to assess PM-related health effects[15].

PMs may include a broad variety of chemical species, ranging from metals to organic and inorganic compounds[16,17]. At this point, sulphate, nitrate, ammonium, carbon, organic chemicals, biological material and metals/minerals generally adsorbed on carbonaceous cores have been known to be the major chemical components of atmospheric PM[18-20]. Among the

55 inorganic compounds, the most important are the trace elements, which are emitted by various
56 natural and anthropogenic sources (crustal materials, road dust, construction activities, motor
57 vehicles, combustion, incineration and other industrial activities)[21-23].

58 PMs and related trace metals have been well documented worldwide. They use to
59 constitute a small fraction of PM mass[14]. Even though, in general, the health risk from
60 potentially toxic metals in urban soils and street dusts are within acceptable levels[24,25], there are
61 some exceptions such as the areas where owing to anthropogenic processes (i.e., mining and
62 smelting plants) metals in PM are often present at concentrations above natural background
63 levels[26].

64 The sampling and analysis of PM is difficult by the complexity of the particle size,
65 particle interactions, chemical partitioning, etc.[27]. In recent years, an increasing concern about
66 PM has favored a growing number of studies that not only include the measurements of its total
67 elemental concentration but also the determination of its chemical form and composition[28,29]. In
68 fact, the chemical and molecular composition represents a key tool for understanding the origin
69 of PM[30] and for characterizing the atmospheric processes in which they are involved[31].
70 Furthermore, it may give important information both on PM toxicological and environmental
71 impact and on mechanisms of PM formation and emission into the atmosphere[32].

72 Non-destructive analytical techniques are a good alternative to the more commonly used
73 high time-consuming destructive analysis[33-35]. For instance, Raman spectroscopy and Scanning
74 Electron Microscopy coupled with Energy Dispersive X-ray microanalysis (SEM-EDX) have
75 been used for the characterization of PM, either stand-alone[36-39] or combined[40-43]. However,
76 since they have not been simultaneously applied, some technical problems appeared (i.e.,
77 particle relocation, movement or beam damage). Hence, a hybrid instrument would transform
78 the spectroscopic characterization of PM into a powerful technique.

79 To avoid these drawbacks, the present research aims to study the viability and
80 effectiveness of direct and non-destructive analytical approaches for a complete characterization
81 (at the micron and submicron levels) of PMs that may pose an important health risk by means of

a newly developed Structural and Chemical Analyser (SCA). This spectroscopic technique combines Raman spectroscopy with SEM-EDX into a unique one allowing us to obtain the SEM, EDX and Raman information on the same micro-spot.

Highly contaminated areas that are abandoned without having taken any preventive action are spaces of high environmental risk that with the time may damage human health. However, establishing a causal link between environmental factors and the adverse health effects, poses many challenges (i.e., bioaccumulation, mobility). Therefore, knowledge of the complex links between environment and health are still insufficient, but are increasing. To achieve this goal is vitally needed the development of sensitive analytical techniques.

The novelty of the SCA presented in this study seeks to answer several questions: what happens to the PM inhaled?; how far can they penetrate?; once in the lung, what happens: are they stable or can they be dissolved?; can they get into the bloodstream, aggravating the problem of metal-rich particles? To provide answers for these questions, several samples were collected in a metal- polluted area. The samples studied were, on the one hand, soils without plant coverage in an abandoned Zn-Pb mine. These soils were selected for being reservoirs of aerodynamic PM that can easily migrate because of the effect of wind. In fact, the lack of vegetation not only facilitates the erosion of the soil itself (vegetation acts as a compacting agent of the soil), but also indicates a high presence of pollutants that difficult the plant germination. In mining areas such zones are indicative of soils highly contaminated with metals and metalloids. Therefore, the aerodynamic PMs derived thereof may pose an important health hazard due to their particle size but even a greater risk may be generated owing to the type of metals that are included in them. On the other hand, lichens were sampled at different distances from the mine in whose surfaces the dust-like PM have been deposited after having been transported. Finally, the stability of the identified PMs was analyzed in the conditions of the alveoli to see what may happen to the PM inhaled into the lungs: if they are/it is retained or are/is able to pass into the bloodstream.

EXPERIMENTAL

Samples and sampling strategy: The work was centered in two kinds of samples collected in an abandoned blende-galena mine described elsewhere[44].

On the one hand, the most likely source of the dust-type PM that is more relevant in the studied area: the non vegetated soils. . Thus, considering that the closer to the polluting activity the higher the metal content in soil, 20 topsoil (first 5 cm) samples were collected at non vegetated areas near the mine entrance and the surrounding tailings. These samples were air dried and sieved to eliminate the coarsest fractions and to facilitate the analysis of the finest particles (Ø<75 μm).

On the other hand, at longer distances ranging from 30 to 600 m, the collected samples were local growing lichens. In an attempt to look for the dust-type PMs that are probably formed from the weathering of the mine wastes and deposited later on, the lichens were sampled at 15 points along the direction of the prevailing winds (north-east). Selected for being more regularly distributed, all the lichens belonged to the Cladoniaceae family. They were carefully taken from tree trunks and rocks to avoid possible cross-contaminations.

Instrumental set-up: Samples were analyzed using a Renishaw's Structural and Chemical Analyzer (SCA) (Renishaw, UK), a combined Scanning Electron Microscope (SEM) and Raman spectrometer. Morphological (from secondary electron image), elemental (from Energy-dispersive X-ray spectroscopy, EDX) and molecular information (from Raman spectroscopy) was obtained at once from the same spot without sample transfer. Thus, this technique enables a comprehensive characterization in a single instrument, what significantly reduces the analysis time and also the errors in the locations of the interest points. Since it does not need any sample relocation or additional pre-treatment once is introduced in the SEM, the elemental and molecular spectra, the SEI (Secondary Electron Image), and the white light images, can be acquired from the same sample position. The data which can be acquired include (1) morphology and mean atomic number from SEM (Secondary Electron Imaging or SEI, and

136 backscatter electron imaging or BEI); (2) elemental composition and distribution map from
137 EDX analysis; (3) chemical composition and identification from Raman spectroscopy; and (4)
138 physical structure (crystallographic and mechanical data) from Raman spectroscopy.

139 First of all, dried samples (soils and lichens) were mounted on clean aluminum stubs
140 with double-sided adhesive graphite tape and coated with gold by means of an Emitech K550x
141 sputter-coater until a 20 nm layer was formed in order to minimize charging effects under SEM
142 imaging conditions.

143 Specimens were observed in a Carl Zeiss EVO-40 SEM equipped with an Oxford
144 Instrument X-Max EDX (Abingdon, UK). The microscope conditions for recording of the
145 morphological information were: high vacuum mode, wolfram hot electron emission and
146 acceleration voltage of 30 kV. For recording of the analytical signal for EDX, the conditions
147 were: probe current varying between 180 pA and 400 pA, work distance of 8.5 mm and X-ray
148 acquisition time of 250 s, in the same microscope conditions described above.

149 The Raman measurements were performed employing an excitation wavelength of 514
150 nm (Modu-Laser) with a nominal power at the source of 50 mW, being the maximum power at
151 the sample of 20 mW. The Raman microscope is connected to the SCA interface with optical
152 fibers. Thus, the power of the laser is attenuated reducing the possibility of photo-
153 decomposition processes. Raman spectra were acquired between 150 and 2000 cm^{-1}, with a
154 spectral resolution of 1 cm^{-1}. In all cases, the integration time was 30 s and the number of
155 accumulations was fixed on 10 in order to enhance the signal to noise ratio.

156 All these features allowed the authors to relate the molecular composition from different
157 points on the surface with the elemental composition, therefore identifying the various
158 component mineral phases in the analyzed particles.

159 **Analytical procedure:** On a first approach, it consisted on the following steps: a)
160 Acquisition of the SEM imaging that enables a comprehensive characterization of particle
161 morphology, including the visualization of the form and the localization of possible inclusions
162 within individual particles. SEM images illustrate different PM types observed in the collected

lichen and soil samples; b) The localization of the different PMs was followed by the definition of the particle size and also by the elemental analysis from EDX either accomplished with manual point analyzer or by mapping. This technique provided the elemental semiquantitative information of a specific PM in percentages or graphically, represented in an EDX spectrum; c) Finally, Raman spectra were collected on those spots to obtain information about the molecular forms that are present in the PM of interest.

Software: Raman data were handled with the Windows®-based Raman Environment software WiRETM®, version 3.2 (Renishaw, UK). Spectral analyses were performed by comparison with spectra from a commercially available spectral library[45]. The elemental composition and mapping obtained with the EDX were analyzed with Microanalysis Suite INCA 4.13 from Oxford instruments.

SEM images were processed with an image processing package, the ImageJ,a public domain, Java-based image processing program developed at the National Institute of Health[46]. To better understand the chemical behavior of the minerals found in the PM at different pH values or environmental conditions, the chemical equilibrium as well as the stability of the molecular forms determined by SCA were evaluated with the MEDUSA software and the HYDRA database of equilibrium constants[47]. The thermodynamic simulations done under the chemical conditions of the mammal lungs[48] tried to determine not only the final, but also the intermediate products of the determined molecular forms, as well as to predict which of them can be introduced into the blood stream after being dissolved in the alveolar fluid or just remain in the alveoli blocking gas exchange.

RESULTS AND DISCUSSION

SEM-EDX: As a first step in the characterization of the PM present in the matrixes studied, the samples were analyzed by SEM-EDX. Focusing the electron beam down to a few nanometers size, the specimens were scanned across, providing an image of the selected area.

190 The image plotted in Figure 1a shows the presence of small-size particles in the studied soils
191 previously sieved (Ø<75 μm) at approximately 650X magnifications, with enough resolution to
192 visualize their morphology. The analysis of such morphology can give the researchers some
193 clues about the physical fragility of those PM that may or may not promote into PMs of smaller
194 size. For instance, some of the particles in Figure 1a with higher size have apparently a stable
195 structure (more unbreakable, probably because they are more crystallized) which may remain
196 without changes due to weathering processes, or be at least more resistant to such phenomena.
197 However, it can be seen that the structure of other particles is not so well-defined and could
198 easily be weathered resulting in a variable number of smaller and more harmful PMs. An
199 example of this is the PM of the Figure 1b, taken from a zoom of Figure 1a, which appear to be
200 weaker. With the time, these PMs could be transported by the wind until being later deposited
201 elsewhere. According to meteorological conditions, the dust-type aerodynamic PMs of Figure 1
202 can migrate long distances and be at the same time weathered into smaller PMs. Figure 1c and
203 1d show, at different magnifications (ranging between 3.2 K and 5.9 K X), the presence of some
204 PMs on lichens surfaces collected downhill the mine at 250 and 400 m, respectively.

205 Particle sizes were also determined by SEM. Depending on the form of the PM, two
206 kinds of measurements were done: the projected area diameter (the diameter of a theoretical
207 circle, which would contain the whole PM) or the Feret's diameter (the longest distance
208 between any two points along the PM boundary). An example of these measurements is
209 indicated in the Figures 1b and 1d, respectively.

210 However, when trying to define the potential hazard of the dust-type PMs derived from
211 the non-vegetated soil that is constantly eroded by the action of wind, rain or snow, a further
212 analysis of the information is required. Size influences the site deposition in the human
213 respiratory tract and the consequent degree of toxicity that may be experienced. Thus, analyzing
214 the SEM images with an image processing tool like ImageJ, the particle size distribution in each
215 image can be deduced. This step allows the researcher to focus on the relevant information, for
216 instance, the particles whose size may pose a health risk. This automation process is very useful

when the number of particles is huge, but it is only possible if the contrast between the particles and the background is enough to choose an optimal threshold to perform a good image binarization. Therefore, this image processing was just done for soil samples (Figure 2a) since the lichens morphology provides a background difficult to remove (see Figure 1d). Figure 2b shows which of the particles present in Figure 2a have a Feret's diameter below 10 μm while Figure 2c represents these particle percentages according to their size. Figure 2b yielded a result of 100 particles with aerodynamic diameters smaller than 10 μm. Almost half of them were classified as PM1.0 and PM2.5 (approximately 47%; see Figure 2c), the most dangerous ones because when inhaled they may reach the peripheral regions of the bronchioles, and interfere with gas exchange in the lungs.

To corroborate the hypothesis that the main origins of PM in this area are the non-vegetated soils, a good approach will be the determination of the chemical composition of PMs. Considering that these soils are found in areas directly affected by the lixiviation of the waste materials from the tailings of the mine activity, they are supposed to be rich in metals, and consequently a great percentage of the PM derived thereof will probably be metal-rich. Figure 3 shows the results of the elemental mapping obtained by using SEM-EDX. This technique provided information about the local chemical composition of the PMs that have been deposited on a lichen surface collected at 300 m from the mine, including lateral heterogeneity within individual particles. This figure represents the reconstruction of maps for some meaningful elements of interest such as copper, sulphur, or lead, even if other hazardous metals (Zn, Fe, Mn, etc.) also showed a wide distribution. The reasons for selecting these elements were: (i) copper is a metal whose presence is relevant and can cause damage to human health when inhaled (Figure 3b); (ii) lead is a metal present in the galena that was extracted from the mine when it was exploited[44] (Figure 3c); and (iii), the presence of sulphur is indicative of both the degree of erosion of the extracted minerals (blende and galena) and the acid mine drainage that is taking place in the area (Figure 3d). Analyzing the information provided by the elemental maps obtained with SEM-EDX, some additional information can also be derived. Looking at

Figures 3c and 3d, it seems that the sulphur presents the same distribution as that of lead. However, it does not necessarily mean that they are always present together, since copper also appears in some smaller areas. When attempting to deduce the molecular information in which these elements have been found, the visualization of this kind of elemental maps may help to some extent. For instance, the maps of Pb and S (Figures 3c and 3d, respectively) give a clue of the probable presence of a lead sulphide (i.e., galena) or lead sulphate that depending on the analyzed area can be pure or present some copper impurities. It also reveals that the impact of the mining activity is still important far from the mine entrance (at even 600 m), due to the weathering of the waste materials that with time are present in particles of smaller size, as those of Figure 3.

Structural and Chemical Analyser (SCA): Although SEM-EDX analysis reveals detailed elemental information, the lack of molecular information of the PMs that often is required is evident, making the analysis of complex heterogeneous compounds particularly challenging. The combination of Raman spectroscopy with SEM-EDX in the same device (SCA unit) has proved to be an ideal tool to characterize at molecular level individual heterogeneous PMs in the fine particle size range.

Figure 4 shows some examples of SCA measurements taken in both a lichen surface (on the left of the image) and a soil sample (on the right). This figure shows the wide variety of possible combinations of the information given by the SCA that provide the researchers with a complete characterization of metal-rich air PM. For the case of lichen, on the one hand, the Raman spectra is illustrated with the elemental maps given by SEM-EDX and, on the other hand, the information of the elemental composition of the PM given by SEM-EDX is shown together with the Raman spectra obtained by SCA. In connection with the PMs, the following information can be obtained from the soil sample: the particle size (Figure 4e), the EDX spectrum (Figure 4d), the Raman spectra (on the top and bottom of the Figure 4) and a zoom of the particle of interest which shows its physical structure or morphology (Figure 4f). The identified minerals at PM level were, among others, siderite ($FeCO_3$), plattnerite (PbO_2) and

271 smithsonite ($ZnCO_3$) shown in Figure 4, as well as dolomite ($CaMg(CO_3)_2$), calcite ($CaCO_3$)
272 and cerussite ($PbCO_3$).

273 A detailed understanding of particle chemistry often requires a combination of
274 analytical methods and measurements. Occasionally, as happens with the some spectroscopic
275 techniques, the SCA technique does not help in the identification of a specific PM but, at least,
276 it helps to identify within a family of minerals. Such can be the case of the PM of the Figure 4a
277 analyzed by SCA. This figure shows the Raman spectrum of a mineral that could not be
278 identified by the WIRETM® software, which only indicated that the mineral studied belonged to
279 the family of the garnets, large group of silicate minerals that share all the same structure of
280 crystals whose chemical formula is $X_3Y_2(SiO_4)_3$[49]. The variety of minerals that can be formed is
281 so large that it is almost impossible to determine which of them corresponds to the Raman
282 spectrum of Figure 4.a without any additional information. In these cases, the elemental maps
283 produced by EDX can help to refine the search to a smaller group of silicates. The element maps
284 showed that the analysed PM was rich in silicon and zinc, concluding that the PM of interest
285 could be a zinc silicate and, consequently, its associated risks may be higher than a non-metallic
286 PM.

287 In SCA it should be noted that the distances that the laser incident and the collected
288 signal have to go over to obtain a Raman spectrum are longer than the usual when this technique
289 is used stand-alone. Therefore, as corroborated in Figure 4, the quality of the Raman spectrum
290 difficultly will reach the quality obtained when using a common Raman spectrometer, although
291 there are exceptions such as the one of Figure 4d. However, there could be other characteristics
292 that should be taken into account. It could happen that according to the purity of the PM
293 analyzed and the effects of the matrix (i.e., organic matter, subtract), the Raman spectrum
294 obtained by SCA may show a higher or lower fluorescence background. This effect is
295 significant in the analysis of PM deposited on lichens (see Figures 4a and 4c), and in the soil
296 PM represented in Figure 4f. Another factor to be considered is the degree of crystallinity of the
297 minerals. When analyzing the morphology of PMs, it can be concluded that a higher degree of

crystallization helps to obtain a better Raman spectrum (especially with narrower band widths). This fact can be observed by comparing Raman spectra shown in Figures 4d and 4f.

When a heterogeneous PM is present (composed by more than single mineral), the combination of such effects can be crucial in the identification of its components. In a noisy spectrum with fluorescence background and non well-defined Raman features, the identification of more than one compound can be really difficult. For that reason the use of elemental information provided by EDX not only may help in the interpretation of the spectra, but also completes the results given by Raman spectroscopy. An example of this is plotted in Figure 4c where the presence of a siliceous compound is only detected by EDX.

In contrast to gaseous specific compounds, the assessment of metal and metalloid compounds in ambient air is complicated by the fact that different species with considerably differing toxicity and/or carcinogenic potential may be encountered. Therefore, to fully evaluate the health effects, it is important to know which species do occur in the environment or at least which compounds form the main constituents. To achieve this goal, SCA has proven to assist greatly in the unambiguous chemical and structural characterization of PMs.

Thermodynamical simulations of the behavior of PMs in the alveoli: With the time, part of the PMs formed in abandoned areas and transported by the air through different distances may be finally breathed by humans or mammals. The proximal cause of a biological response to PM is due to the dose deposited at the target site rather than the external exposure. Characterization of the exposure-dose-response continuum for PMs requires an understanding of the mechanistic determinants of inhaled particle dose. Furthermore, dosimetric information is critical for extrapolating human health effects based on animal toxicological studies[50].

The dose of inhaled PMs to the respiratory tract is governed by a number of factors [50-52]. Dose to a target tissue depends on the initial deposition and subsequent retention of particle within the respiratory tract. In general terms, the particles with aerodynamic diameters over 10 μm are deposited in the extrathoracic region (nasal and oral passages), the PM ranging from

PM10 to PM2.5 in the tracheobronchial region (trachea and bronchioles) while PM<2.5 μm can reach the alveolar region (alveoli).

Given that the smaller the PM the greater the damage generated (because they can penetrate deeper into the respiratory tract), this study aimed to interpret what may happen at the alveolar level to the PM2.5 and PM1 that were characterized by SCA. To achieve this goal chemical equilibrium models were developed with the help of MEDUSA software based on the information provided by SCA and simulating the conditions of the mammal's alveolus itself[48]. At this point it should be highlighted that is pretty difficult to define the total concentration of a given solid in some environments, such as lungs. Thus, the diagrams of Figure 5 are represented in a way that allows the researcher to work with different total concentrations of the studied components.

Figure 5 summarizes some results obtained in the chemical simulations done for the cases of lead and zinc. Although the pH values that are represented range from 4 to 9, the grey shaded areas are indicative of the pH values which will not be (under any physiological condition) compatible with human life[53]. According to WHO reports, human exposure to lead is estimated to account 0.6% of the global burden of disease since this cumulative toxicant affects multiple body systems[54]. Even if a major source of exposure to lead comes from inhalation, nowadays laboratories primarily assess lead exposure with whole blood lead measurements[55]. The dissolution of zinc containing PMs have also the potential to be absorbed into the bloodstream and transported to the heart where it may well produce changes in cardiac function by altering the normal gene expression of some proteins[56]. Consequently, it would be interesting to define if the lead and zinc present in the different minerals found by SCA are able or not to reach the bloodstream.

As mentioned above, the major ores extracted were sphalerite and galena, both sulphide minerals of zinc and lead respectively. It is well known that when the mine wastes are pilled in tailings at open air their molecular composition may remain unchanged over time or can suffer several weathering processes that finally lead to a change in the molecular composition of the

352 mineral.Therefore, several chemical simulations were done starting not only from the original
353 ores, but also from the weathering products previously identified by SCA. Such simulations
354 demonstrated that sulphide containing PMs may easily degrade to sulphate, carbonate or oxide
355 due to several reactions, not only under environmental conditions, but also under the human
356 physiological conditions.

357 When the first takes place and the original ores are disaggregated into small PMs
358 preserving its chemical configuration, once inhaled they may suffer any chemical modification
359 since the human physiological conditions are not necessarily the same as those of the natural
360 environment.

361 The simulations done with plattnerite (see Figure 5a) showed that it can be dissolved if
362 not completely at least partially. In relation to these simulations it can be said that the behavior
363 of this lead (IV) oxide in the lungs is dose-dependent. At low and normal concentrations (less
364 than 10^{-4} mM) the PbO_2 is completely dissolved in the lung fluids allowing its access into the
365 bloodstream as lead tetrahydroxide. This kind of situations could be reached under acute
366 exposures (characterized by their low exposure time). Unfortunately, these are the most
367 unconscious and common form of exposition to hazardous substances since whoever it is
368 exposed is not aware of the potential risks it poses. However, when the plattnerite levels are
369 very high (concentrations higher than the previously mentioned) it can be partially dissolved,
370 approximately 10% of the total concentration of PbO_2. This extreme situation may be achieved
371 under chronic exposures.

372 Figure 5b represent the behavior of the galena, which is neither dose nor pH- dependent
373 and in all simulated cases remains almost completely in the solid form in the range of
374 physiological pH (in lungs and blood) that is compatible with the life. Since they remain
375 practically insoluble in the lungs liquid, the risks associated to these PMs would preferentially
376 be focused at alveolar level for interfering gas exchange.

377 The case of the sphalerite, however, is completely different because its behavior besides
378 being dose-dependent is also pH-dependent, showing higher solubility when the pH of the

379 medium increases (see Figure 5c and d). At higher concentrations (chronic exposures) and at the
380 pH values characteristic of blood (approx. 7.4), the fraction of the soluble compounds (Zn^{2+} +
381 $ZnOH^{+}$ + $ZnHCO_3^{+}$) achieves the 28% of the total Zn concentration. The simulations done with
382 smithsonite ($ZnCO_3$), which is commonly formed from the weathering of sphalerite in kastic
383 environments, came one with the trend of sphalerite PMs.

384 When comparing the mobility of both metals, it can be noted that from the
385 thermodynamical point of view zinc compounds are more labile than the lead ones, since the
386 soluble fraction of the chemical compounds responsible for that solubility are higher in all
387 cases. The Zn mobility depends on a large amount of parameters (Zn^{2+} and Cl^{-} concentration,
388 pH, etc.) and, therefore, any variation in the external conditions implies more relevant changes
389 in its chemical distribution.

390 The access of the PM to the bloodstream via dissolution-reprecipitation processes or direct
391 transference as a solid phase imply a wider distribution of the metal in the body causing not
392 only cardiovascular effects but also neurological diseases.

393

394 **CONCLUSIONS**

395

396 The presented work shows that a comprehensive characterization of atmospheric
397 particles can only be obtained using a complementary combination of different analytical
398 methods, ranging from microscopic properties of individual particles to an advanced chemical
399 characterization of complex molecules comprising PM. At this point it should be highlighted
400 that the results of this research have proved the viability and effectiveness of direct and non-
401 destructive analytical methods for a complete characterization of PMs that may pose important
402 health risks. Furthermore, SCA that has been firstly applied in PMs during this research, has
403 demonstrated the complementary of the two techniques into a unique one for the
404 characterization of the PMs directly in the environmental matrixes where they were deposited.

The analytical procedure followed has supplied highly valuable information required to interpret the influence of PM on pollution phenomena.

Summarizing, it could be noted that: (i) the results obtained came one with the idea which pointed to the non-vegetated soils as the main air pollutant in the studied area (ii) the development of this analytical methodology (SCA together with the chemical simulations) and its applications presents both challenging and good opportunities for future research in the study of air PMs; (iii) the information obtained in this study is crucial for evaluating the chemistry and physical properties of PMs related to human health; (iv) the simulation processes done by MEDUSA helps to understand whether the finest PMs that reach the alveoli may or may not dissolve in the alveoli liquid, promoting not only respiratory diseases, but also cardiovascular or neuronal damages.

ACKNOWLEDGEMENTS

The Basque Government through the Berrilur III project (Ref. IE09-0242) has financially supported this work. N. Goienaga acknowledges her pre-doctoral fellowship from the UPV/EHU. Technical and human support provided by the Raman-LASPEA Laboratory of the SGIker (UPV/EHU, MICINN, GV/EJ, ERDF and ESF) is gratefully acknowledged.

REFERENCES

(1) Desauziers, V. *Trends*. **2004**, 23, 252- 260.

(2) Osornio-Vargas, A. R.; Serrano, J.; Rojas-Bracho, L.; Miranda, J., García-Cuellar, C.; Reyna, M. A.; Flores, G.; Zuk, M.; Quintero, M.; Vázquez, I.; Sánchez-Pérez, Y.; López, T.; Rosas, I. *Chemosph*. **2011**, 83, 618-626.

(3) Sawyer, K.; Mundandhara, S.; Ghio, A. J.; Madden, M. C. *J. Toxicol. Environ. Helath, Part A.* **2010**, 73, 41-47.

(4) D'Almeida, G. A.; Koepke, P.; Shettle, E. P. *Atmospheric Aerosols: Global Climatology and Radiative Characteristics.* Deepak, A. Publishing, Hampton, VA, **1991**.

(5) Park, K.; Cho, G.; Kwak, J. *Aerosol Sci. Technol*. **2009,** 43, 375-386.

(6) Hollaway, T., Fiore, A.; Hastings, M. G. *Environ. Sci. Technol.* **2003**, 37, 4535-4542.

(7) Artinano, B.; Salvador, P.; Alonso, D. G.; Querol, X.; Alastuey, A. *Environ. Pollut.* **2003**, 125, 453-464.

(8) Bogo, H.; Otero, M., Castro, P.; Ozafran, M. J.; Kreiner, A.; Clavo, E. J.; Negri, R. M. *Atmos. Environ*. **2003**, 37, 1135-1147.

(9) Querol, X.; Alastuey, A.; Rodriguez, S.; Viana, M.; Arginano, B.; Salvador, P.; Mantella, E.; García do Santos, S.; Fernandez Patier, R.; de La Rosa, J.; Sanchez de la Campa, A., Menendez, M.; Gil, J. J. *Sci. Total Environ*. **2004**, 359-376.

(10) Pope, C. A. III; Burnett, R. T.; Krewski, D.; Jerrett, M.; Shi, Y.; Calle, E. E.; Thun, M. J. *Circulation*. **2009**, 120, 941-948.

(11) Raaschou-Nielsen, O.; Andersen, Z.; Hvidberg, M.; Jensen, S. S.; Ketzel, M.; SØrensen, M.; Loft, S.; Overvad, K.; TjØnneland, A. *Environ. Health Perspect*. **2011**, 19, 860-865.

(12) WHO. Health Aspects of Air Pollution with Particulate Matter, Ozone and Nitrogen Dioxide. Report on a WHO working group, Bonn, Germany. **2003**.

(13) Oberdörster, G. *Math. Phys. Engin. Sci*. **2000**, 358, 2719-2740.

(14) Park, K.; Cho, G.; Kwak, J. Aerosol Sci. Technol. 2012, 43, 375-386.

(15) Dergham, M.; Lepers, C.; Verdin, A.; Billet, S.; Cazier, F.; Courcot, D.; Shirali, P.; Garçon, G. *Chem. Res. Toxicol*. **2012**, 25, 904-919.

(16) Park, S. S.; Kim, Y. J. *Chemosph*. **2005**, 59, 217-226.

(17) Dubey, B.; Pal, A. K.; Singh, G. *Atmosph. Pollut. Res*. **2012**, 3, 238-246.

(18) Baulig, A.; Singh, S.; Marchand, A.; Schins, R.; Barouki, R.; Garlatti, M.; Marano, F.; Baeza-Squiban, A. *Toxicology*. **2009**, 26, 126-135.

(19) Danielsen , P. H.; MØller, P.; Jensen, K. A.; Sharma, A. K.; Wallin, H. *Chem. Res. Toxicol*. **2011**, 24, 168-184.

(20) McMurry, P. H.; Shepherd, M.; Vickery, J. *Particulate Matter Science for Policy Makers: A NARSTO Assessment*. Cambridge University Press, New York, **2004**.

(21) Arditsoglou, A.; Samara, C. *Chemosph.* **2005**, 59, 669-678.

(22) Shah, M. H.; Shaheen, N. *Atmosph. Res*. **2010**, 95, 201-223.

(23) Carrero, J.A., Arrizabalaga, I., Goienaga, N., Arana, G., Madariaga, J.M., 2012. *Traffic Related Metal Distribution Profiles and their Impact on Urban Soils*. Springer, Dordrecht, **2012**.

(24) Lu, Y.; Yin, W,; Huang, L. B.; Zhang, G. L.; Zhao, Y. G. *Environ. Geochem. Health*. **2011**, 33, 93-102.

(25) Betha, R.; Balasubramanian, R. *Atmosph. Environ*. **2011**, 45, 5273-5281.

(26) Zheng, N.; Liu, J. H.; Wang, Q. C.; Liang, Z. Z. *Sci. Tot. Environ*. **2010**, 408, 726-733.

(27) Spurny, K. R. Ed. *Analytical Chemistry of Aerosols*. Lewis Publishers: Boca Ratón, FL, **1999**.

(28) Magas, O. K.; Gunter, J. T.; Regens, J. L. Environ. Sci. Pollut. Res. 2007, 14, 19-23.

(29) Wild, P.; Bourgkard, E.; Paris, C. *Method Molec. Bio*. **2009**, 472, 139-167.

(30) Weinbruch, S.; Ebert, M.; Gorzawski, H.; Dirsch, T.; Berq, T.; Steinnes, E. *J. Environ. Monitor*. **2010**, 12, 1064-1071.

(31) Grupta, A. K.; Karar, K.; Srivastava, A. *J. Hazar. Mat*. **2007**, 14, 19-23.

(32) Astolfi, M. L.; Canepari, S.; Cardarelli, E.; Ghinghi, S.; Marzo, M. L. *Ann. Chim*. **2006**, 96, 183-194.

(33) Bings, N. H.; Bogaerts, A.; Broekaert, J. A. C. *Anal. Chem*. **2012**, DOI: 10.1021/ac3031459.

(34) Horan, A. J.; Gao, Y.; Hall IV, A. H.; Johnston, M. V. *Anal. Chem*. **2012**, 84, 9253-9258.

(35) Domingos, J. S. S.; Regis, A. C. D.; Santos, J. V. S.; de Andrade, J. B.; da Rocha, G. O. *J. Chromat. A.* **2012**, 1266, 17-23.

(36) Odziemkowski, M.; Koziel, J. A.; Irish, D. E.; Pawliszyn, J. *Anal. Chem*. **2001**, 73, 3131-3139.

(37) Lee, A. K. Y.; Chan, C. K. *Atmosph. Environ*. **2007**, 41, 4611-4621.

(38) Potgieter-Vermaak, S. S.; Van Grieken, R. *Appl. Spectroc*. **2006**, 60, 39-47.

(39) Vargas Jentzsch, P.; Ciobota, V.; Kampe, B.; Rösch, P.; Popp, *J. Raman Spectrosc*. **2012**, 43, 514-519.

(40) Stefaniak, E. A.; Worobiec, A.; Potgieter-Vermaak, S.; Alsecz, S.; Van Grieken, R. *Spectrochim. Acta B*. **2006**, 61, 824-830.

(41) Worobiec, A.; Potgieter-Vermaak, S.; Brooker, A.; Darchuk, L.; Stefaniak, E.; Van Grieken, R. *Microchem*. **2010**, 94, 65-72.

(42) Potgieter-Vermaak, S.; Van Grieken, R. *Spectros. Europe*. **2010**, 22, 12-16.

(43) Choeel, M.; Debout, K.; Flament, P.; Lecornet, G.; Perdrix, E. Sobanska, S. *Atmosph. Environ*. **2006**, 40, 4439-4449.

(44) Goienaga, N.; Arrieta, N.; Carrero, J. A.; Olivares, M.; Sarmiento, A.; Martinez-Arkarazo, I.; Fernández, L. A.; Madariaga, J. M. *Spectrochim Acta A*. **2011**, 80, 66-74.

(45) RRUFF Downs, R. T. *The RRUFF Project: an integrated study of the chemistry, crystallography, Raman and infrared spectroscopy of minerals.* Program and Abstracts of the 19th General Meeting of the International Mineralogical Association in Kobe, Japan. **2006**, O03-13.

(46) Collins, T. J. *BioTechn*. **2007**, 43, S25-S30.

(47) Puigdomenech, I. KTH Royal Institute of Technology, Department of Chemistry, MEDUSA (Make Equilibrium Diagrams Using Sophisticated Algorithms) Webpage: http://www.kemi.kth.se/medusa/

(48) Nielson, D. W.; Goerke, J.; Clements, *J. A. Proc. Natl. Acad. Sci. USA*. **1981**, 78, 7119-7123.Kidwell, C. B.; Ondov, J. M. *Aerosol Sci. Technol*. **2001**, 35, 596-601.

(49) U.S.E.P.A. Air Quality Criteria for Particulate Matter. EPA/600/P95/004aF-cF, Springfield, VA. **1996**.

(50) Kim, C. S. *Resp. Care*. **2000**, 45, 695-711.

(51) Broday, D. M.; Georgopoulus, P. G. *Aerosol Sci. Technol*. **2001**, 34, 144-159.

(52) WHO. *Global Health Risks: Mortality and Burden Disease Attributable to Selected Major Risks*. Geneva, **2009**.

(53) Ng, A. W.; Bidani, A.; Heming, T. A. *Lung*. **2004**, 182, 297-317.

(54) WHO. *Exposure to Lead: A Major Public Health Concern*. Genova, **2010**.

(55) Schütz, A.; Bergdahl, I. A.; Ekholm, A.; Skerfving, S. *Occupational and environmental medicine*. **1996**, 53, 736-740.

(56) Graff, D. W.; Cascio, W. E.; Brackhan, J. A.; and Devlin, R. B. *Environ. Health Perspec*. **2004**, 112, 792-798.

FIGURE CAPTIONS

1.- Figure 1. EDX (left) and SEM (right) images at different low (below 700 X) and high magnifications (over 3 K X) of soils (**a** and **b**) and lichen surfaces (**c** and **d**).

2.- Figure 2. (a) Image of a non-vegetated soil; **(b)** Representation of the particles of the previous image whose Feret's diameter is below 10 μm; **(c)** Feret's diameter average diagram.

3.- Figure 3. (a) Site of interest in a lichen surface for the elemental mapping of: **(b)** copper; **(c)** lead; **(d)** sulphur.

4.- Figure 4. Two areas of interest analyzed by SCA: a lichen surface as organic matrix **(b)** and a soil sample as an inorganic matrix **(e)**. **(a)** Raman spectrum plus elemental map; **(c)** Raman spectrum plus compositional analysis; **(d)** Raman plus EDX spectra; **(f)** Raman spectrum plus morphology of an analysed PM.

5.- Figure 5. MEDUSA simulations done with the mineral phases identified by SCA: galena **(a** and **b)** and sphalerite **(c** and **d)**. The grey shaded areas indicate the pH values incompatible with human life.

FIGURE 1

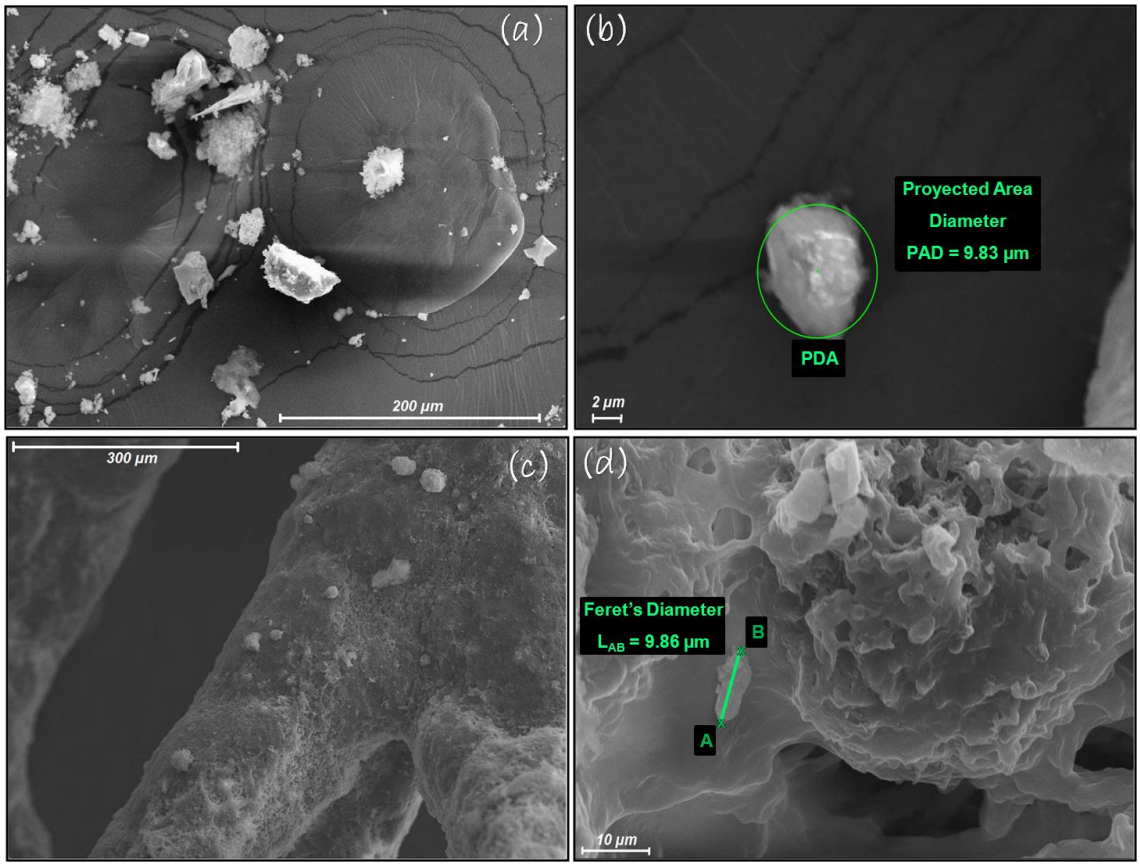
(a)
200 µm
(b)
Proyected Area
Diameter
PAD = 9.83 µm
PDA
2 µm
300 µm
(c)
(d)
Feret's Diameter
L_{AB} = 9.86 µm
B
A
10 µm

574

575

576

577

578 **FIGURE 2**

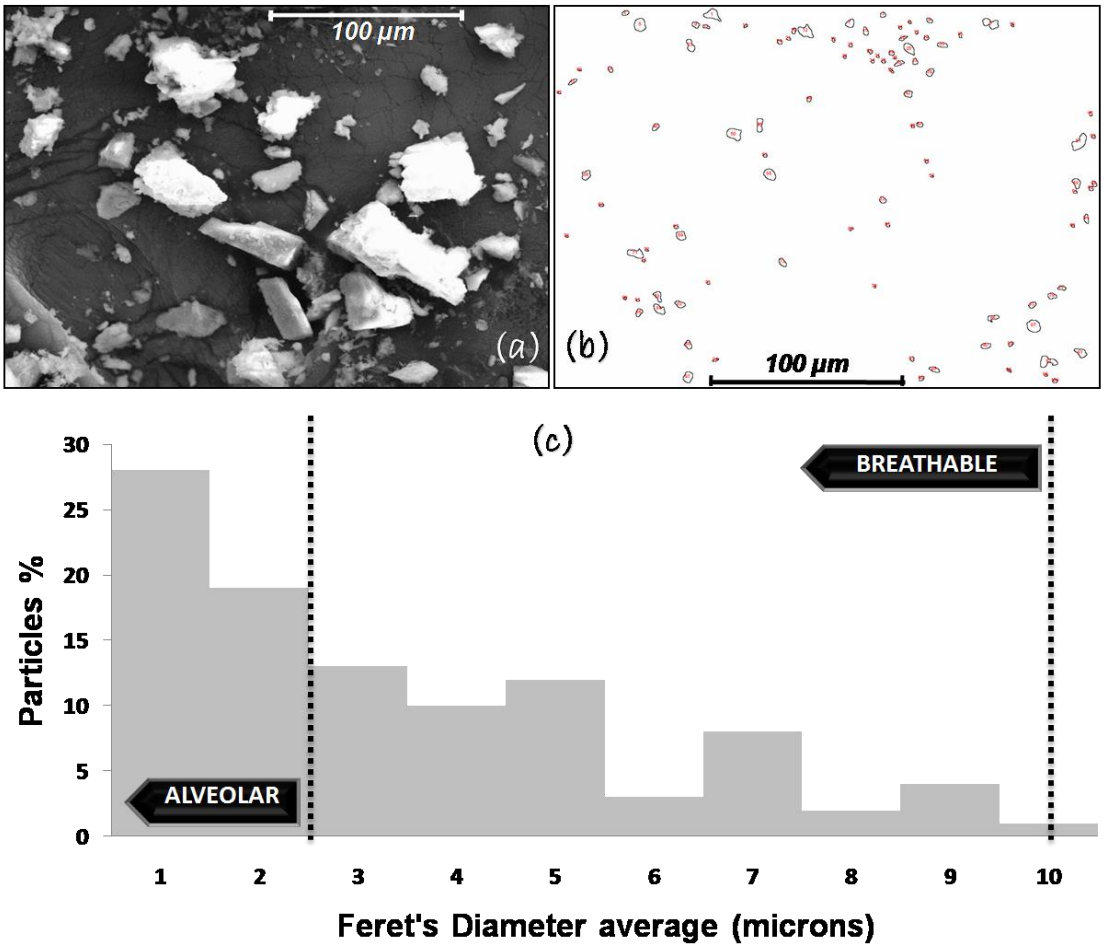

579

580

581

582

583

584

585

586

587 **FIGURE 3**

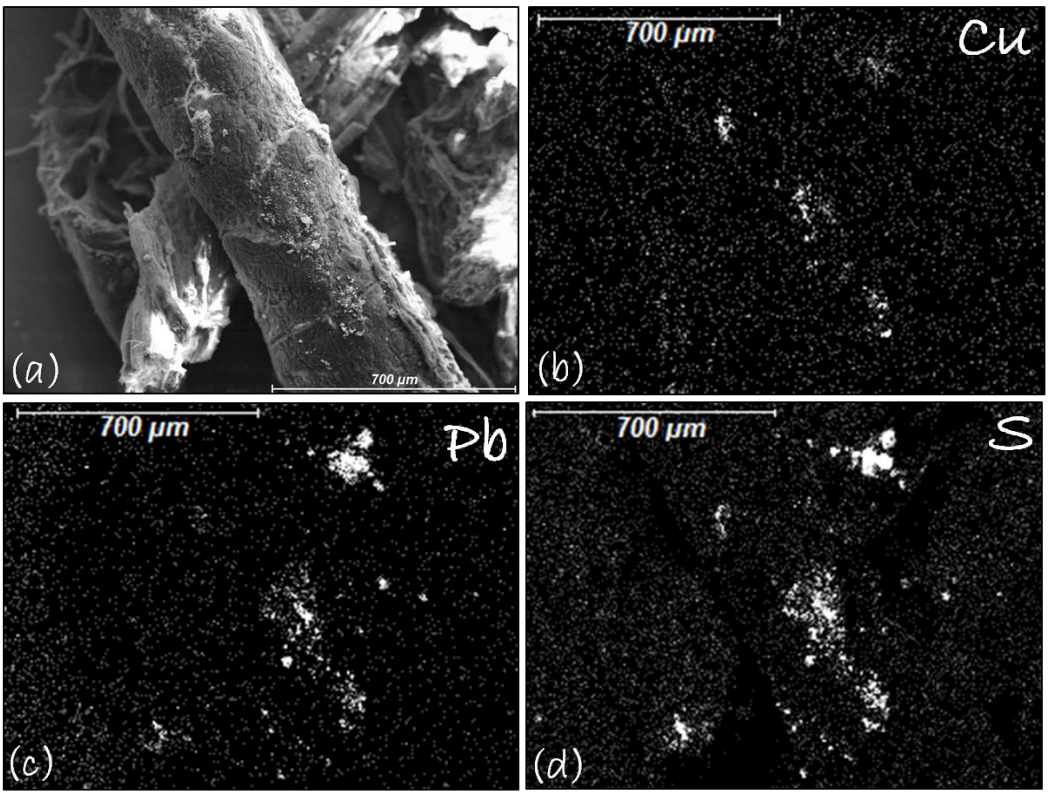

588

589

590

591

592

593

FIGURE 4

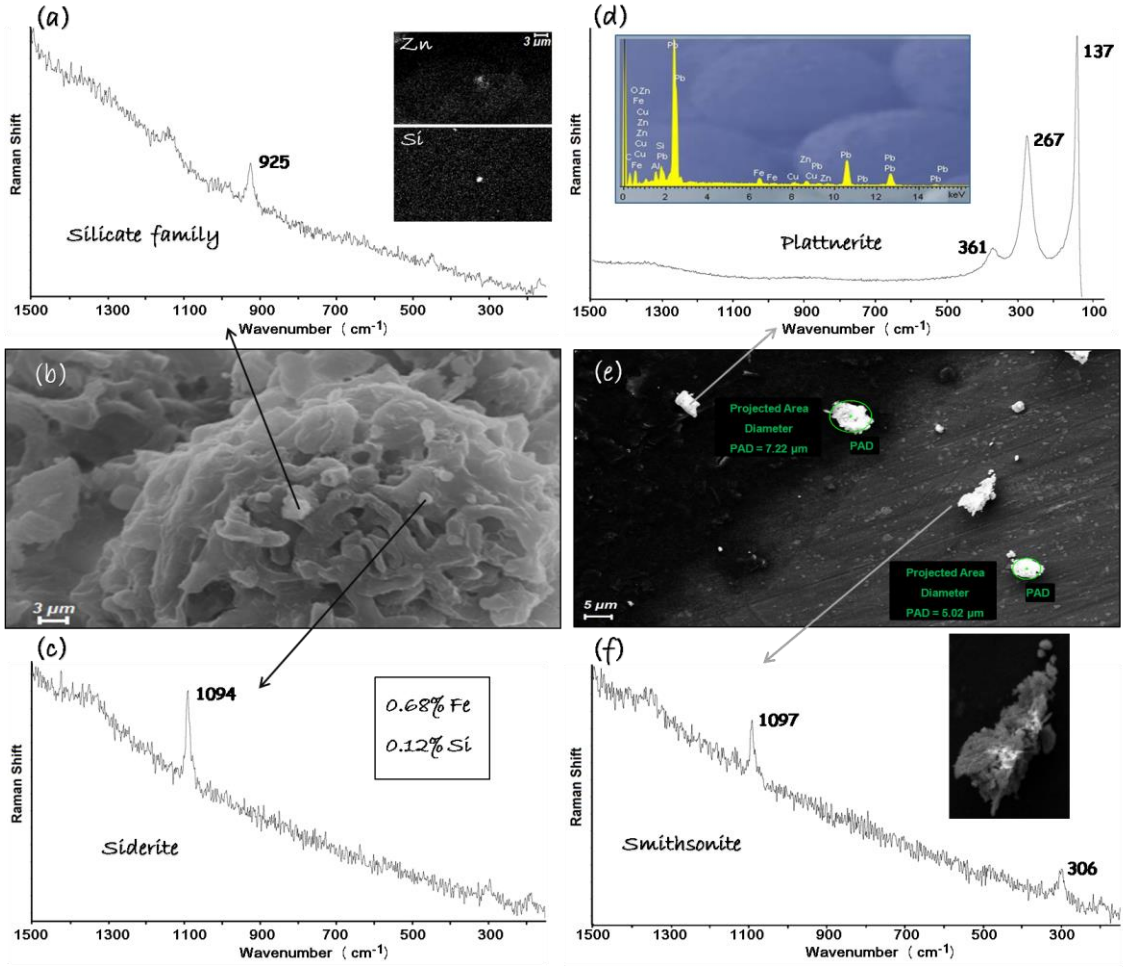
(a)
Zn
3 μm
Si
925
Silicate family
Raman Shift
1500 1300 1100 900 700 500 300
Wavenumber (cm-1)
(d)
137
267
361
Plattnerite
1500 1300 1100 900 700 500 300 100
Wavenumber (cm-1)
(b)
3 μm
(e)
Projected Area
Diameter
PAD = 7.22 μm
PAD
Projected Area
Diameter
PAD = 5.02 μm
PAD
5 μm
(c)
1094
0.68% Fe
0.12% Si
Siderite
1500 1300 1100 900 700 500 300
Wavenumber (cm-1)
(f)
1097
Smithsonite
306
1500 1300 1100 900 700 500 300
Wavenumber (cm-1)

FIGURE 5

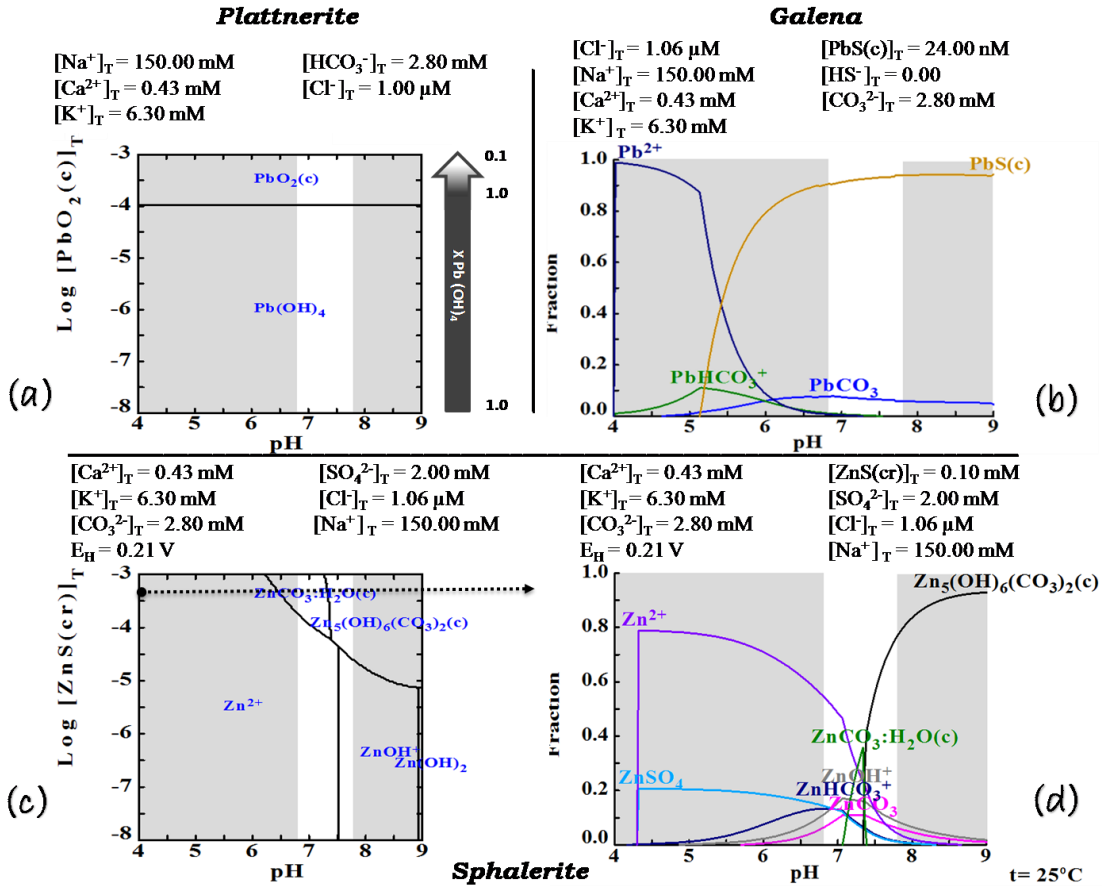
Plattnerite
Galena
(a)
(b)
(c)
(d)
Sphalerite
t= 25°C
pH
Fraction
Log [PbO2(c)]T
Log [ZnS(cr)]T
PbO2(c)
Pb(OH)4
X Pb (OH)4
Pb2+
PbS(c)
PbHCO3+
PbCO3
ZnCO3:H2O(c)
Zn5(OH)6(CO3)2(c)
Zn2+
ZnOH+
Zn(OH)2
ZnSO4
ZnHCO3+
ZnCO3

613

614

615

616

617

618 **TOC**

619

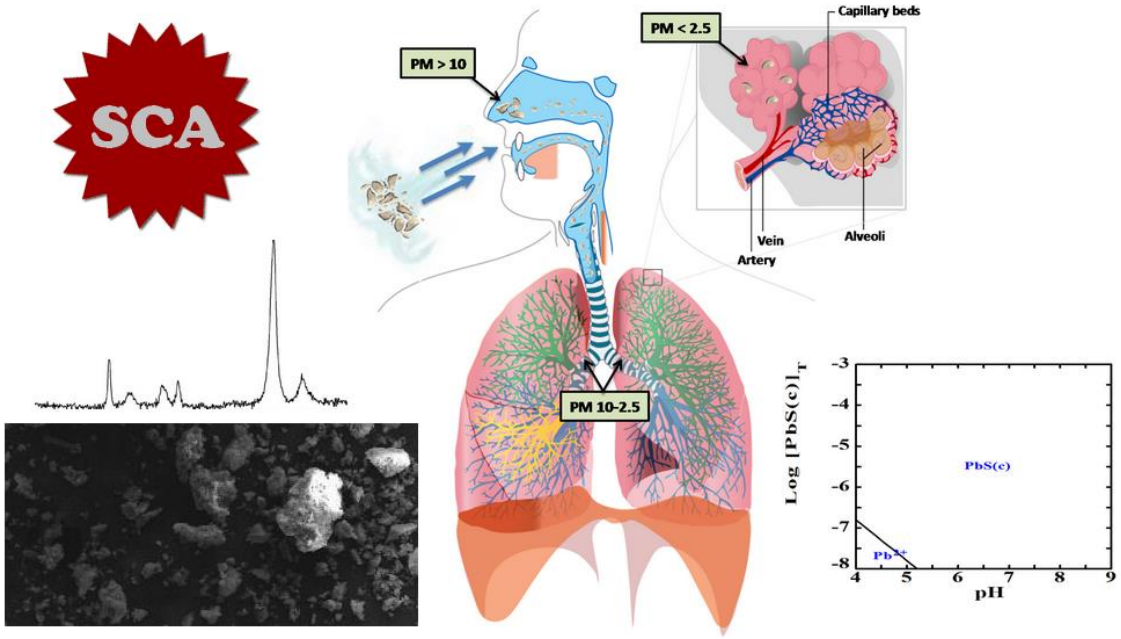

620